

# Identification and Characterization of a Neutralizing Monoclonal Antibody for the Epitope on HM-1 Killer Toxin

Dakshnamurthy Selvakumar<sup>1</sup>, Qing-Zhu Zhang<sup>1</sup>, Masahiko Miyamoto<sup>1</sup>,  
Yasuhiro Furuichi<sup>2</sup> and Tadazumi Komiyama<sup>1,\*</sup>

<sup>1</sup>Department of Biochemistry, Faculty of Pharmaceutical Sciences, Niigata University of Pharmacy and Applied Life Sciences, 5-13-2 Kamishinei-cho, Niigata 950-208; and <sup>2</sup>GeneCare Research Institute Co. Ltd., 200 Kajiwara, Kamakura 247-0063

Received November 28, 2005; accepted December 17, 2005

**Killer toxin-neutralizing monoclonal antibody (nmAb-KT) against HM-1 killer toxin (HM-1) produced by yeast *Williopsis saturnus* var. *mrakii* IFO 0895 reduces both the killing and glucan synthase inhibitory activity of HM-1. nmAb-KT is classified as IgG1( $\kappa$ ) and has been shown to be ineffective against HYI killer toxin produced by the related yeast *W. saturnus* var. *saturnus* IFO 0117. To determine the epitope for nmAb-KT, overlapping peptides were synthesized from the primary structure of HM-1. nmAb-KT reacted with peptides P5 (<sup>33</sup>NVHWMVTGGST<sup>43</sup>), P6 (<sup>39</sup>TGGSTDGKQG<sup>48</sup>) and P7 (<sup>44</sup>DGKQGCATIWE<sup>56</sup>), which represent the middle region of the HM-1 sequence. P6 reacted most strongly with nmAb-KT. Combined analysis by immunoblotting, surface plasmon resonance (SPR) analysis and yeast growth inhibition assay showed that nmAb-KT recognizes a specific epitope within peptide P6. The  $K_d$  value of nmAb-KT against HM-1 and P6 were determined to be  $5.48 \times 10^{-9}$  M and  $1.47 \times 10^{-6}$  M by SPR analysis, respectively. These results strongly indicate that nmAb-KT binds to HM-1 at the sequence <sup>41</sup>GSTDGK<sup>46</sup>, and not to HYI at the same position. The potential active site of HM-1 involved in the killing activity against sensitive yeast is discussed.**

**Key words:** epitope identification,  $\beta$ -1,3-glucan synthase, HM-1 killer toxin, neutralizing monoclonal antibody, SPR analysis.

Abbreviations: HM-1, HM-1 killer toxin; HYI, HYI killer toxin; nmAb-KT, HM-1 killer toxin neutralizing monoclonal antibody; SPR, surface plasmon resonance; ELISA, enzyme-linked immunosorbent assay; TBS, 20 mM Tris-HCl (pH 7.5) containing 150 mM NaCl; TBS-T, 20 mM Tris-HCl (pH 7.5) containing 150 mM NaCl and 0.05% Tween 20.

Several fungi, especially yeasts, can produce proteinaceous killer toxins that are lethal to other taxonomically related or unrelated sensitive microorganisms, and can represent a sophisticated biological mechanism of competition in natural ecosystems (1). Species of *Williopsis* (2, 3) produce killer toxins that kill other sensitive yeast strains (4–7). HM-1 and HYI are strong yeast killer toxins produced by yeasts *W. saturnus* var. *mrakii* IFO 0895 and *W. saturnus* var. *saturnus* IFO 0117 (5, 6), which were previously known as *Hansenula mrakii* and *H. saturnus*, respectively (2).

HM-1 belongs to the K9-killer toxin group (4), and consists of 88 amino acids, of which 10 are cysteine (8). It is inactivated by reducing agents, such as 2-mercaptoethanol and dithiothreitol, suggesting that S-S bonds forming tertiary structures maintain the structure and biological activity of HM-1 (7). HM-1 is stable against heat treatment (100°C, 10 min) and a wide range of pH values (pH 2.0–11.0). The isoelectric point of HM-1 is pH 9.1 and the molecular mass is calculated to be 9,500 daltons from the amino acid sequence (8). The three-dimensional structure of HM-1 has been determined by nuclear

magnetic resonance spectroscopy (9), and the HM-1 gene has been cloned from chromosomal DNA of HM-1-producing yeasts (10).

HYI consists of 87 amino acids and its molecular mass is about 9,500 Da (11). The isoelectric point of HYI is pH 5.8, and it is stable when heated at 60°C for 1 h and at pH 5.0 to 8.0 at 30°C for 24 h (6). Most of these features of HYI are similar to HM-1 except the isoelectric point and local amino acid sequences. Amino acid homology predicts that HM-1 is larger than HYI by one amino acid that is absent from HYI, corresponding to position 43 in HM-1 (11). Although, HM-1 and HYI show a small local difference in primary structure, the overall homology is 87% (10, 11), and the mechanism of killing action against sensitive yeasts by inhibiting  $\beta$ -1,3-glucan synthase activity is shared by the two toxins (12, 13).

The killer-toxin neutralizing monoclonal antibody (nmAb-KT) binds HM-1 and neutralizes the yeast killing activity of HM-1 (8). However, we previously prepared the HM-1-specific monoclonal antibodies 1F1 and 4A2, which bind to HM-1, but they did not neutralize the yeast killing activity of HM-1 (14). In this study, we investigated the epitope of HM-1 recognized by nmAb-KT using various synthetic overlapping peptides of HM-1 and HYI. The binding affinities of nmAb-KT for HM-1, HYI, HM-1 peptides and HYI peptide were compared by the effect on yeast growth, immunoblot blot analysis, sandwich

\*To whom all correspondence should be addressed. Tel: +81-25-268-1223, Fax: +81-25-268-1230, E-mail: tkomiyam@niigata-pharm.ac.jp

enzyme-linked immunosorbent assay (ELISA) and surface plasmon resonance (SPR) analysis. The epitope of HM-1 recognized by nmAb-KT was clearly identified. We believe this is the first report of the binding characteristics and mapping of the epitope site of yeast killer toxins as characterized by SPR and dot blotting analysis.

#### MATERIALS AND METHODS

**Materials**—Affinity purified nmAb-KT was prepared from the hybridoma clone of 6207 (8), and polyclonal rabbit anti-serum against HM-1 was prepared by Technology Incubation & Transfer Ltd. (Saitama, Japan) and Nippon Bio-Test Laboratories, Inc. (Tokyo, Japan). Purified HM-1 and HYI were prepared in our laboratory as previously described (6, 11, 13, 15). A mouse monoclonal antibody isotyping kit was purchased from Amersham Biosciences Co. Ltd., (Tokyo, Japan). Horseradish peroxidase-conjugated anti-mouse goat IgG and alkaline phosphatase conjugated anti-mouse goat IgG were obtained from Sigma (St. Louis, MO, USA). The BIAcore X system, CM5 sensor chip and amine coupling kit were the products of Biacore AB (Uppsala, Sweden). Peptides were synthesized by Sigma Genosys Co. Ltd., Japan. To identify the sequence of the epitope for nmAb-KT, thirteen synthetic overlapping HM-1 peptides (P1–P13) were prepared from the N-terminus of the primary structure of HM-1 (Table 1). In addition to these peptides, one HYI nanopptide representing the amino acid sequence of positions 39–47 of HYI was synthesized. YPD medium consisted of 1% yeast extract and 2% each of peptone and glucose.

**Antibody Isotyping**—The isotyping of nmAb-KT was determined using an antibody isotyping kit according to the manufacturer's protocol. Briefly, an isotyping stick was incubated with 3 µg/ml of nmAb-KT in 20 mM Tris-HCl (pH 7.5) containing 150 mM NaCl (TBS) for 15 min at room temperature with agitation. The stick was washed with TBS containing 0.05% Tween-20 (TBS-T), and incubated with horseradish peroxidase-conjugated anti-mouse goat IgG for 15 min at room temperature with shaking.

Table 1. Overlapping peptides used to determine the epitope for nmAb-KT.

Peptide name	Peptide sequence
HM-1 peptides	
P1	<u>1</u> GDGYLIMCKNCDPN <sup>14</sup>
P2	<u>9</u> KNCDPNTGSCDWQNWNT <sup>26</sup>
P3	<u>22</u> QNWNTCVGIGA <sup>32</sup>
P4	<u>27</u> CVGIGANVHWMV <sup>38</sup>
P5	<u>33</u> NVHWMVTGGST <sup>43</sup>
P6	<u>39</u> TGGSTDGKQG <sup>48</sup>
P7	<u>44</u> DGKQGCATIWEGS <sup>56</sup>
P8	<u>49</u> CATIWEGSGCVGRSTT <sup>64</sup>
P9	<u>60</u> GRSTTMCCPA <sup>69</sup>
P10	<u>65</u> MCCPANTCCN <sup>74</sup>
P11	<u>70</u> NTCCNINT <sup>77</sup>
P12	<u>73</u> CNINTGFYIRS <sup>83</sup>
P13	<u>78</u> GFYIRSYRRVE <sup>88</sup>
HYI nanopptide	<u>39</u> TGESNGQQG <sup>47</sup>

Numbering of the peptide is based on the HM-1 amino acid sequence. Overlapping residues are underlined. Numbering of the amino acid positions is from the N-terminal amino acid.

Then, 4-chloro-1-naphthol in cold methanol and 0.1% hydrogen peroxide were added to identify the isotyping of nmAb-KT.

**Killing Activity of HM-1 and HYI with nmAb-KT**—The killing activities of the HM-1 and HYI proteins were measured using a liquid culture method described previously (12). Approximately  $4 \times 10^6$  cells/ml of *Saccharomyces cerevisiae* A451 were incubated in YPD medium containing 15 µg/ml of nmAb-KT or 40 ng/ml of HM-1 or HYI, or nmAb-KT combined with HM-1 or HYI, at 30°C for 8 h. Yeast growth was measured by absorbance at 600 nm.

**Preparation of Membrane Fractions of *S. cerevisiae***—Membrane fractions of *S. cerevisiae* were prepared by a method described previously (16) with some modifications. Cells of *S. cerevisiae* A451 in the mid-exponential phase and collected by centrifugation were washed with 1 mM ethylene diamine tetraacetate (EDTA) and suspended in breaking buffer consisting of 50 mM Tris-HCl (pH 7.5), 0.5 M NaCl, 1 mM EDTA and 1 mM phenylmethanesulfonyl fluoride. The cells were disrupted with glass beads by vortexing and centrifuged for 5 min at  $1,000 \times g$  at 4°C. The supernatant was centrifuged at  $100,000 \times g$  for 30 min at 4°C. The membrane fraction obtained was homogenized in membrane buffer consisting of 50 mM Tris-HCl (pH 7.5), 10 mM EDTA, 1 mM β-mercaptoethanol and 33% glycerol, and stored at –80°C.

**Measurement of β-1,3-Glucan Synthase Activity**—β-1,3-Glucan synthase assay was performed according to the method of Cabib and Kang (16). The reaction mixture consisted of 5 mM UDP-D-[U-<sup>14</sup>C]glucose, 75 mM Tris-HCl (pH 7.5), 0.75% bovine serum albumin, 25 mM KF, 0.75 mM EDTA, 20 µM guanosine 5'-[γ-thio]triphosphate and 10 µl of the membrane fraction of *S. cerevisiae* in a total volume of 40 µl. The reaction was started by adding the membrane fraction, and the mixture was incubated at 30°C for 60 min. To measure the effect of nmAb-KT on β-1,3-glucan synthase activity, 15 µg/ml of nmAb-KT or 2 µg/ml of HM-1 or HYI, or nmAb-KT combined with HM-1 or HYI, was added before the addition of the membrane fraction. The reaction was stopped by adding cold 250 µl 10% trichloroacetic acid, and the mixture was incubated on ice for 10 min, and then filtered through glass microfibre filters (Whatman GF/B). The filters were washed four times with 250 µl of cold 10% trichloroacetic acid, and further washed twice with 250 µl 95% ethanol. The radioactivity retained on the filters was counted in a liquid scintillation counter.

**Sodium Dodecyl Sulfate–Polyacrylamide Gel Electrophoresis (SDS-PAGE) and Western Blotting**—The HM-1 and HYI proteins (each 0.1 µg) were separated in a 15% polyacrylamide gel by electrophoresis, and the proteins were transferred onto a ProBlott membrane (Applied Biosystem) using a semi-dry electroblotting apparatus. The membrane was blocked for 1 h in TBS-T supplemented with 4% non-fat dry milk, and then incubated for 2 h with 3 µg/ml of nmAb-KT in blocking solution. The membrane was washed three times with TBS-T, and then further incubated with alkaline phosphatase-conjugated anti-mouse goat IgG for 1 h. The membrane was washed and the proteins on the membrane were visualized by adding Western blue (Promega) as a substrate. A prestained broad range standard was used as a marker.

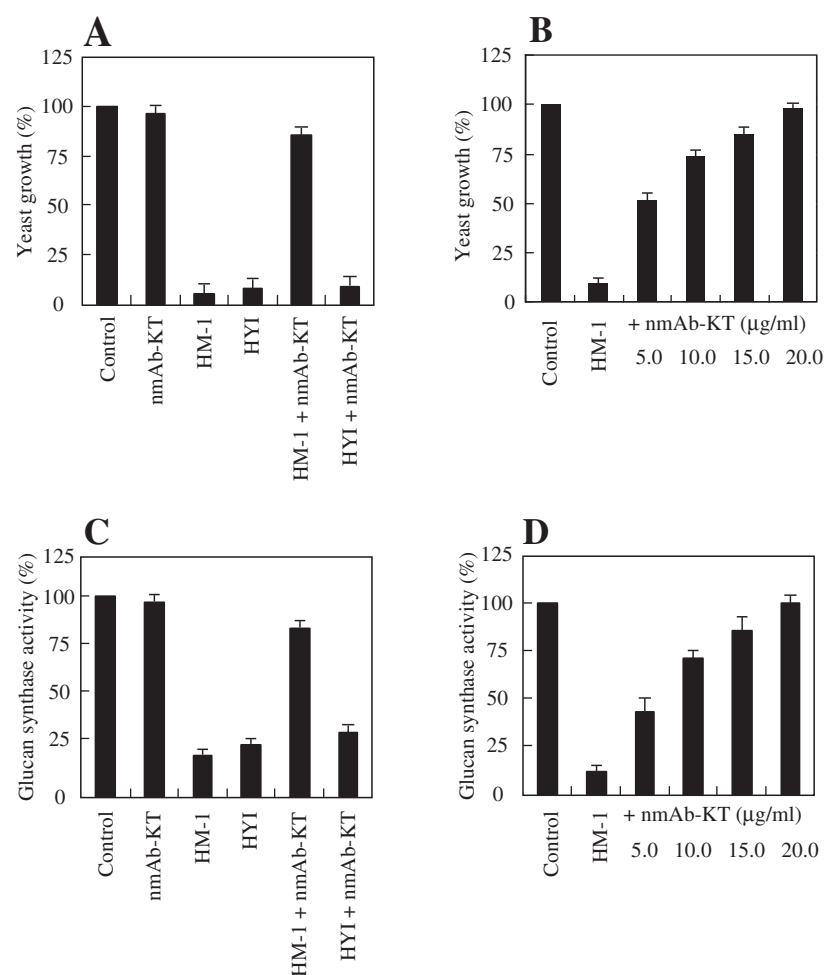


**Fig. 1. Effect of nmAb-KT.** (A) Effect on yeast growth and killing activity of HM-1 and HYI, (B) Dose dependence of the nmAb-KT neutralizing activity on the yeast growth and killing activity of HM-1, (C) Effect on  $\beta$ -1,3-glucan synthase activity and inhibitory activity of HM-1 and HYI. (D) Dose dependence of the nmAb-KT neutralizing activity on the  $\beta$ -1,3-glucan synthase inhibitory activity of HM-1. Assay methods and conditions are described in "MATERIALS AND METHODS." Activity is expressed relative the control sample without nmAb-KT, HM-1 and HYI taken as 100%. Data represent the percentage means of three experiments  $\pm$  SE.

**SPR Analysis of HM-1 and HYI**—Real-time measurement of the interaction between nmAb-KT and HM-1 or HYI was done using a BIAcore X biosensor system at 25°C. In the immobilization experiments, HBS-EP buffer [10 mM HEPES, 150 mM NaCl, 3 mM EDTA, 0.005% polysorbate 20 (pH 7.4)] was used as the eluent buffer at a flow rate of 10  $\mu$ l/min. Immobilization of nmAb-KT on a CM5 sensor chip was achieved by the standard amine coupling method except for the activation. Briefly, 35  $\mu$ g/ml of nmAb-KT diluted in 10 mM sodium acetate (pH 5.0) was injected into the biosensor surface, which was activated with a 1:1 mixture of 120  $\mu$ l of 200 mM *N*-ethyl-*N'*-(3-dimethylaminopropyl)carbodiimide hydrochloride and 50 mM *N*-hydroxysuccinimide, and then 120  $\mu$ l of 1 M ethanolamine (pH 8.5) was injected to inactivate the unreacted reagents. Nearly 3,000 resonance units of nmAb-KT were immobilized. One channel of each sensor chip treated in the same way without nmAb-KT was used as a control for the nonspecific binding of HM-1 or HYI to the carboxymethylated dextran surface. Purified HM-1 and HYI proteins were analyzed at a concentration of 6.25–100 nM. After each measurement, the chip surface was regenerated with 20  $\mu$ l of 1 M HCl. HM-1 overlapping peptides and the HYI nanopeptide were analyzed at a concentration of 500 nM. Peptide P6 was analyzed at a concentration of 31.3–500 nM. After each measurement, the chip

surface was regenerated with 6  $\mu$ l of 10 mM HCl. Kinetic sensorgram curves were evaluated with BIAevaluation 3.0 to find the association rate constant,  $k_{on}$ , and dissociation rate constant,  $k_{off}$ . The dissociation constant,  $K_d$ , was calculated from the equation  $K_d = k_{off}/k_{on}$ .

**Peptide Analysis by Growth Inhibition Assay**—To determine the effect of overlapping HM-1 peptides and HYI nanopeptide on yeast growth, approximately  $4 \times 10^6$  cells/ml of *S. cerevisiae* A451 were incubated in YPD medium containing 10  $\mu$ M of each peptide or 4.21 nM of HM-1 or peptide P6 combined with different concentrations of nmAb-KT at 30°C for 8 h. Yeast growth was measured by the absorbance at 600 nm.

**Peptide Binding Analysis by Dot Blotting**—ProBlott membranes were placed in a dot blotting apparatus (Bio-craft Inc), and the defined areas were coated with 0.1  $\mu$ g each of the thirteen synthetic overlapping HM-1 peptides or the HYI nanopeptide. The membranes were blocked with 2% non-fat dry milk in TBS for 1 h at room temperature, washed with TBS-T, incubated with nmAb-KT as the primary monoclonal antibody for 2 h at room temperature, and then washed three times with TBS-T. Bound peptides were detected by incubating the membranes with a 1:5,000 dilution of alkaline phosphatase conjugated anti-mouse goat IgG for 1 h at room temperature, followed by staining with Western blue.

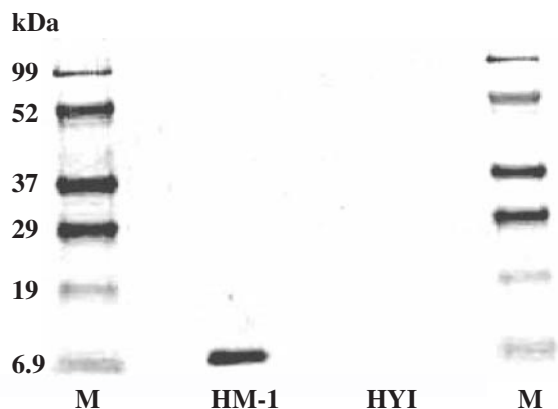


Fig. 2. **Western blot analysis of HM-1 and HYI.** Purified HM-1 and HYI were subjected to electrophoresis, electroblotted and detected using nmAb-KT as the primary antibody as described in "MATERIALS AND METHODS." M: molecular weight standards (lanes 1 and 4), HM-1 (lane 2), and HYI (lane 3).

## RESULTS

**Characterization of nmAb-KT**—nmAb-KT was classified as IgG1( $\kappa$ ) by a mouse monoclonal antibody isotyping kit. Because the typing characterization reveals an antibody structure, its use might be desirable for some applications including immunological techniques. SDS-PAGE showed only heavy and light chain bands with molecular masses of about 57 kDa and 25 kDa, respectively, indicating the purity of the antibody. Adding nmAb-KT to a yeast culture resulted in the yeast retaining 96.4% of growth, but the addition of HM-1 and HYI caused marked inhibition of yeast growth to 5.8% and 8.2% respectively (Fig. 1A). Including nmAb-KT with HM-1 produced an 85% recovery in yeast growth, but including nmAb-KT with HYI produced no recovery (9.0% growth), even at a concentration 15  $\mu$ g/ml nmAb-KT. Adding nmAb-KT resulted in 97.3% on  $\beta$ -1,3-glucan synthase activity being retained, but HM-1 and HYI reduced  $\beta$ -1,3-glucan synthase activity to 20.8% and 26.0% of control, respectively (Fig. 1C). Including nmAb-KT with HM-1 produced a maximum recovery of  $\beta$ -1,3-glucan synthase activity to 87.3%, but including nmAb-KT with HYI produced a low recovery to 32%, even at a concentration 15  $\mu$ g/ml nmAb-KT. Our studies show the dose dependence of nmAb-KT on yeast killing activity (Fig. 1B) and  $\beta$ -1,3-glucan synthase inhibitory activity (Fig. 1D). The data also strongly suggest that nmAb-KT can neutralize the killing and inhibitory activities of  $\beta$ -1,3-glucan synthase by HM-1 specifically, and that it does not interfere with either activity of HYI, even though the primary structures of HM-1 and HYI share a high degree of homology (10, 11).

**Binding Specificities of nmAb-KT by Western Blot Analysis**—Figure 2 shows a clear single band corresponding to the expected molecular mass of about 9,500 Da for HM-1, but HYI did not show a band on the membrane. These results indicate that nmAb-KT binds only to HM-1, and not to HYI. The same result was also obtained by the dot blotting method (data not shown).

**SPR Analysis of HM-1 and HYI**—The binding specificities and kinetic parameters of purified HM-1 and HYI were determined by SPR analysis. Biacore sensorgrams showed

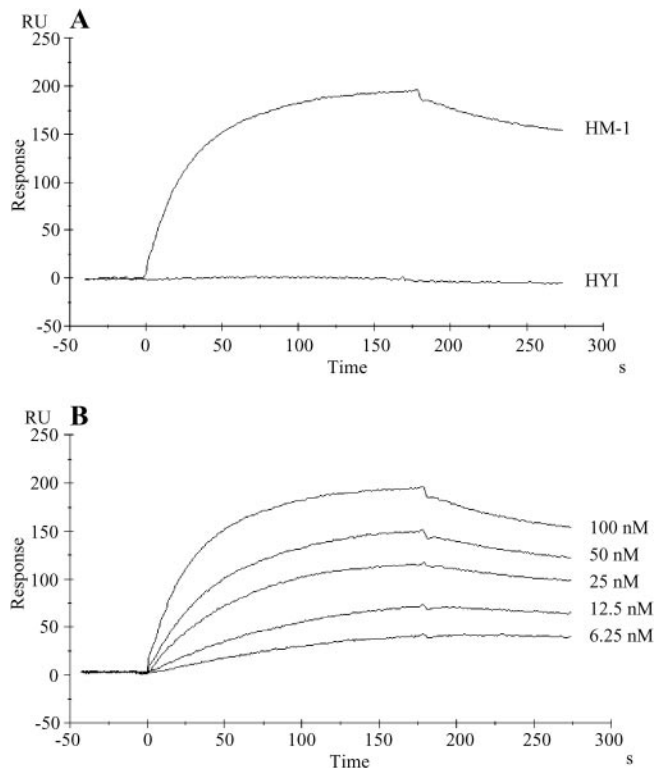


Fig. 3. **SPR analysis of HM-1 and HYI.** Preparation of immobilized nmAb-KT on CM5 sensor chips and the analytical methods are described in "MATERIALS AND METHODS." (A) Association and dissociation of HM-1 and HYI at 100 nM. (B) HM-1 signals at different concentrations in the range of 6.25–100 nM. RU: resonance units.

Table 2. **Kinetic parameters for the binding of nmAb-KT to HM-1 and HYI as measured by SPR analysis.**

Analyte	$k_{on}$ ( $\times 10^5$ $M^{-1} s^{-1}$ )	$k_{off}$ ( $\times 10^{-3}$ $s^{-1}$ )	$K_d$ ( $\times 10^{-9}$ M)
HM-1	3.3	1.81	5.48
HYI	ND	ND	ND

The kinetic constants for HM-1 and HYI were determined using a Biacore biosensor:  $k_{on}$ , association rate constant;  $k_{off}$ , dissociation rate constant;  $K_d$  value was calculated as  $K_d = k_{off}/k_{on}$ . ND, signals not detected.

the degree of interaction between immobilized nmAb-KT and HM-1 or HYI (Fig. 3, A and B). The kinetic data from SPR analysis showed that HM-1 has a strong binding affinity for nmAb-KT, while HYI shows no binding to nmAb-KT. Table 2 shows the calculated values of  $k_{on}$ ,  $k_{off}$  and  $K_d$ . The  $K_d$  value of HM-1 is  $5.48 \times 10^{-9}$  M. Therefore, we can conclude that nmAb-KT shows strong reactivity toward HM-1, but not toward HYI.

**SPR Analysis of HM-1 Peptides**—The binding specificities and kinetic parameters of synthetic overlapping HM-1 peptides and the HYI nanopeptide were determined by SPR analysis. Among the thirteen synthetic overlapping HM-1 peptides, P1 is the first ( $^1$ GDGYLIMCKNC $DPN^{14}$ ) and P13 the last ( $^{78}$ GFYIRSYRR $VE^{88}$ ) in the HM-1 molecule (Table 1). The Biacore sensorgrams showed the degree of interaction between immobilized nmAb-KT and HM-1 peptides or the HYI nanopeptide. Kinetic data from SPR

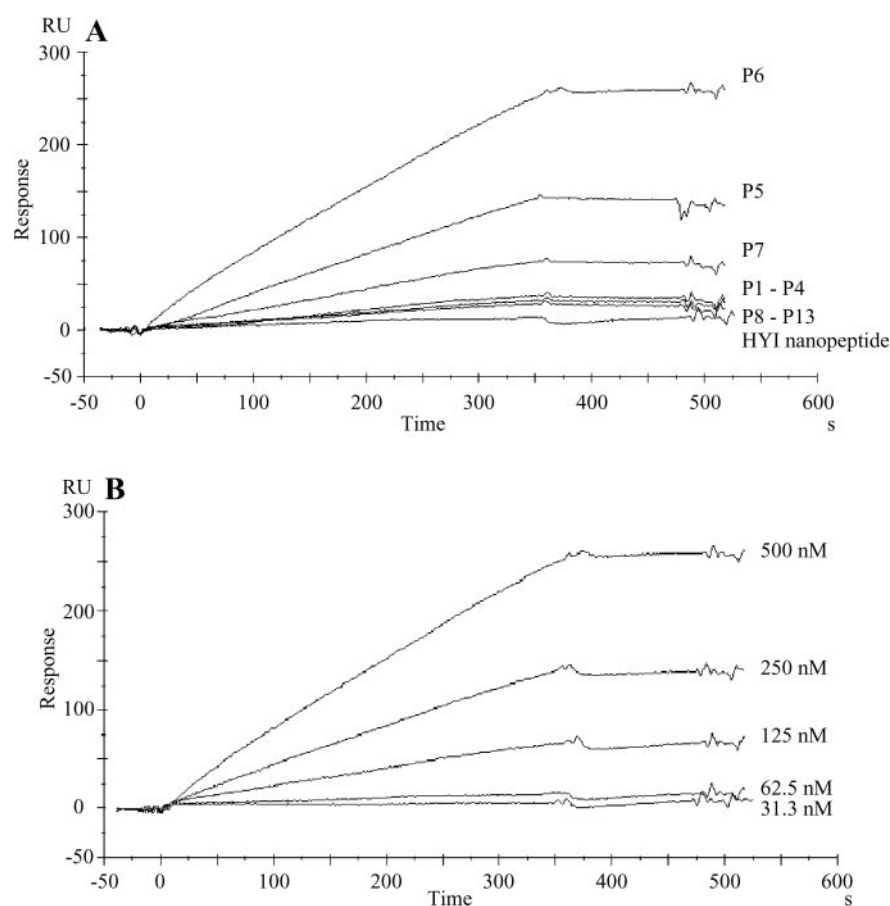


**Fig. 4. SPR analysis of HM-1 overlapping peptides and the HYI nanoepitope.** Preparation of immobilized nmAb-KT on CM5 sensor chips and the analytical methods are described in “MATERIALS AND METHODS.” (A) Interaction between nmAb-KT and thirteen HM-1 overlapping peptides or HYI nanoepitope at 500 nM. (B) Peptide P6 signals at different concentrations in the range of 31.3–500 nM.

**Table 3. Kinetic parameters for the binding of nmAb-KT to HM-1 peptide P6 and HYI nanoepitope as measured by SPR analysis.**

Analyte	$k_{\text{on}}$ ( $\times 10 \text{ M}^{-1} \text{ s}^{-1}$ )	$k_{\text{off}}$ ( $\times 10^{-4} \text{ s}^{-1}$ )	$K_{\text{d}}$ ( $\times 10^{-6} \text{ M}$ )
HM-1 peptide P6	4.72	6.92	1.47
HYI nanoepitope	ND	ND	ND

The kinetic constants of HM-1 peptide P6 and HYI nanoepitope were determined using a Biacore biosensor:  $k_{\text{on}}$ , association rate constant;  $k_{\text{off}}$ , dissociation rate constant;  $K_{\text{d}}$  value was calculated as  $K_{\text{d}} = k_{\text{off}}/k_{\text{on}}$ . ND, signals not detected.

analysis showed that HM-1 peptide P6 ( $^{39}\text{TGGSTDGKQG}^{48}$ ) has a marked binding affinity for nmAb-KT and the neighboring peptide P5 ( $^{33}\text{NVHWMVTGGST}^{43}$ ), and that P7 ( $^{44}\text{DGKQGCATIWEGS}^{56}$ ) has a weaker binding affinity for nmAb-KT (Fig. 4A). The HYI nanoepitope, corresponding to the same position in HYI as HM-1 peptide P6 (11), showed no signals that indicated binding to nmAb-KT (Fig. 4A). Because of these results, peptide P6 was examined more closely at different concentrations to determine the precise kinetic parameters (Fig. 4B). Table 3 shows the calculated values of  $k_{\text{on}}$ ,  $k_{\text{off}}$  and  $K_{\text{d}}$ . The  $K_{\text{d}}$  value of HM-1 peptide P6 is  $1.47 \times 10^{-6} \text{ M}$ . These results strongly confirm that nmAb-KT recognizes peptide P6 position in HM-1.

**Peptide Analysis of nmAb-KT**—Peptide analysis of nmAb-KT was performed by yeast growth inhibition assays. All thirteen overlapping peptides and the HYI nanoepitope had little effect on yeast growth, except the

P5, P6 and P7 peptides, which showed greater inhibition of yeast growth (Fig. 5A). The killing activity of P6 blocked in a dose-dependent manner by the addition of nmAb-KT (Fig. 5B), indicating that peptide P6 reacts with nmAb-KT. Because the strong inhibitory effect of peptide P6 was reduced by nmAb-KT, P6 could be the specific epitope for nmAb-KT.

**Dot Blotting Analysis**—To investigate the epitope for nmAb-KT in the HM-1 molecule, the binding specificities of nmAb-KT to thirteen synthetic overlapping HM-1 peptides and the HYI nanoepitope were analyzed by dot blot analysis (Fig. 6). Among thirteen overlapping peptides tested, peptides P5, P6 and P7 showed strong binding to nmAb-KT (Fig. 6A). Figure 6B shows the strongest binding specificities of peptide P6 with nmAb-KT, while the HYI nanoepitope, corresponding to the same position in HYI, showed no binding to nmAb-KT. This result is in good agreement with the SPR analysis, which indicated that the epitope for nmAb-KT is localized within HM-1 at positions 39–48.

## DISCUSSION

The identification and characterization of the epitope of an antibody that neutralizes killing activity is inevitably important to understanding the structure and function of the relationship of the killer toxin, and for the use of killer proteins or antibodies in agriculture and the clinical field. Yamamoto *et al.* (8) raised an nmAb-KT that can

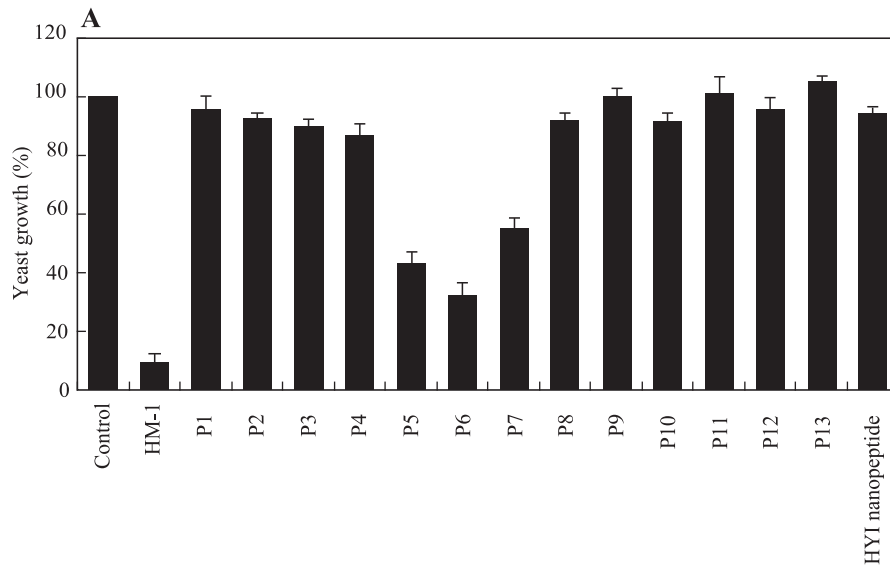


**Fig. 5. Peptide analysis of nmAb-KT.** The growth inhibition assays and assays of the killing activity of HM-1 overlapping peptides are described in "MATERIALS AND METHODS." (A) Effect of HM-1 peptides and the HYI nanopeptide on *S. cerevisiae* A451 growth. (B) Dose dependence of neutralizing effect of nmAb-KT on the killing activity of P6. Activity is expressed relative to the control sample without peptide and nmAb-KT taken as 100%. Data represent the percentage means of three experiments  $\pm$  SE.

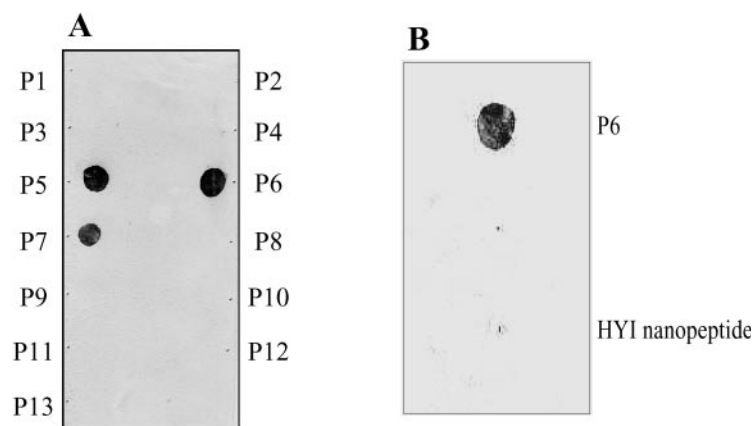
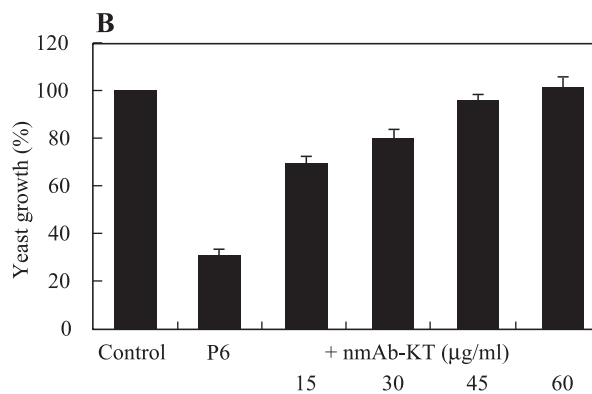


**Fig. 6. Peptide binding assay by dot blotting analysis.** Dot blotting and detection using nmAb-KT as a primary antibody are described in "MATERIALS AND METHODS." (A) Thirteen overlapping peptides adsorbed on the membrane. (B) HM-1 peptide P6 and HYI nanopeptide adsorbed on membrane.

neutralize the killing activity of HM-1. Killer toxins by themselves have been proposed as potential fungistatic agents (17, 18). However, the protein and immunogenic nature of killer toxins have hampered their direct application to eradicating systemic infections of pathogenic fungi. Whether the anti-fungal activity of a given killer toxin is strong enough to control the growth of pathogenic organisms effectively is not clear, and whether injected killer toxins have anti-fungal efficacy over a long period against

immune responses is also doubtful. Recently, using recombinant DNA technology and a phage display system, we applied nmAb-KT for idiotype vaccination to produce anti-idiotypic antibodies that mimic the internal image of HM-1 (manuscript submitted). We were successful in obtaining single-chain fragment variable anti-idiotypic antibodies that showed strong fungicidal activity against various clinically important pathogens. Our preliminary studies also showed that another killer toxin, HYI, despite its

close similarity to HM-1 in structure and glucan synthase inhibitory activity, is not neutralized by nmAb-KT. Our results prompted us to characterize the active site of HM-1 responsible for the expression of the killing activity and the epitope site bound by nmAb-KT.

In this study we generated a new sandwich ELISA method using nmAb-KT, so that small amounts of HM-1 could be quantitated more precisely (data not shown). We then characterized the epitope of HM-1 recognized by nmAb-KT that neutralizes the killing and glucan synthase inhibitory activity of HM-1 (Fig. 1, A and C). The nmAb-KT neutralization effect on yeast killing and glucan synthase inhibitory activity by HM-1 were analyzed precisely by observing the dose dependence of nmAb-KT, and these results confirmed that nmAb-KT strictly binds and neutralizes the killing and inhibitory activities of HM-1 (Fig. 1, B and D). Scanning analysis of synthetic overlapping HM-1 peptides by growth inhibition assays showed that peptide P6 and its neighboring peptides have marked killing activity on yeast growth (Fig. 5A). The nmAb-KT neutralization effects on yeast killing activity by P6 were analyzed precisely by observing the dose dependence of nmAb-KT, and these results indicated that nmAb-KT binds and neutralizes the killing activity of P6 (Fig. 5B). These combined observations strongly confirm that the nmAb-KT epitope lies within HM-1 peptide P6 (<sup>39</sup>TGGSTDGKQG<sup>48</sup>), which could be part of the active site of the HM-1 killer function. Consistently, HYI, which is not neutralized by nmAb-KT, contains a dissimilar amino acid sequence <sup>39</sup>TGESNGQQG<sup>47</sup> in the corresponding region, and shows only about 50% local homology to HM-1. Noteworthy is that HYI differs from HM-1 only in the <sup>39</sup>TGESNGQQG<sup>47</sup> region, despite its overall homology being as high as 87%. SPR analysis showed that nmAb-KT binds HM-1 with a high affinity ( $K_d = 5.48 \times 10^{-9}$  M), but does not bind to HYI (Fig. 3, A and B; Table 2).

In addition to this study, we tried spot analysis, in which synthetic peptides are covalently linked to a membrane filter using an oligopeptide spacer (19), to find the epitope recognized by nmAb-KT. We synthesized and analyzed 39 peptides comprising 12 amino acid residues with 10 residues overlapping the next peptide and linked to the membrane by two  $\beta$ -alanine spacers (14), but we detected no positive spot with nmAb-KT. The most probable explanation is that steric hindrance caused by the covalent linkage of the peptides to the membrane filter may prevent the binding of large molecules such as nmAb-KT.

In this study, we used soluble peptides to identify the epitope position on HM-1 for nmAb-KT. From the binding ability of nmAb-KT and the homology between HM-1 and HYI, we propose the nmAb-KT epitope to be as follows. In addition to P6, overlapping peptides P5 and P7 bound strongly to nmAb-KT. Amino acids <sup>39</sup>TG<sup>40</sup> and <sup>47</sup>QG<sup>48</sup> in P6 are homologous, respectively, to <sup>39</sup>TG<sup>40</sup> and <sup>46</sup>QG<sup>47</sup> in the HYI nanopeptide (Table 1). Therefore, considering that a general protein epitope consists of 5 - 6 amino acid residues, we propose the epitope for nmAb-KT to be at the position <sup>41</sup>GSTDGK<sup>46</sup> in HM-1. Also, molecular modeling of HM-1 using RasMol software (Fig. 7) showed sequence 41–46 protruding from the surface of the HM-1 molecule (9), and residues, G-41, T-43, D-44 and K-46 in <sup>41</sup>GSTDGK<sup>46</sup> are different from the corresponding residue in HYI.

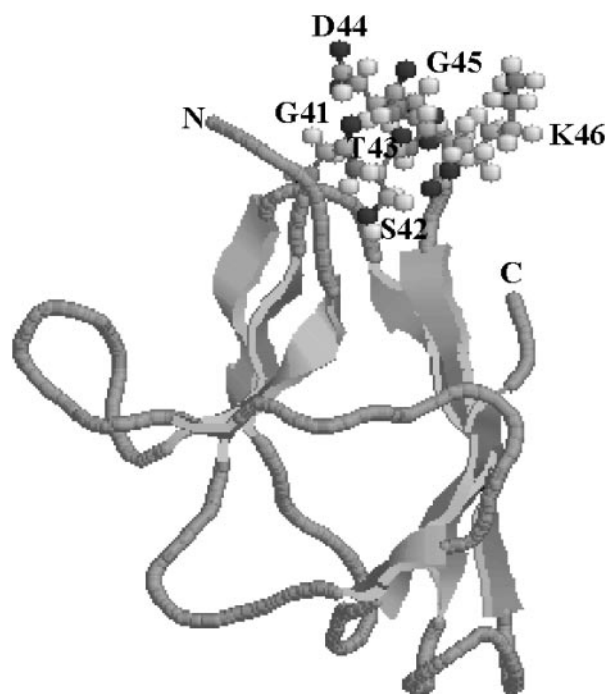


Fig. 7. **Three-dimensional structure of HM-1.** Image showing the three-dimensional structure of HM-1 drawn using RasMol software. The binding epitope for nmAb-KT in positions 41–46 is shown as balls and sticks. N and C indicate the N-terminus and C-terminus of HM-1, respectively.

Peptide binding assays showed that nmAb-KT reacts most strongly with HM-1 overlapping peptide P6, but not with the HYI nanopeptide (Fig. 6, A and B). Peptide and nmAb-KT binding analyses carried out by SPR analysis showed that HM-1 peptide P6 binds to nmAb-KT with a calculated  $K_d = 1.47 \times 10^{-6}$  M, but that the HYI nanopeptide showed no signals for nmAb-KT (Fig. 4, A and B; Table 3). These results suggest that HM-1 overlapping peptide P6 is an active site for the expression of the killing activity of HM-1. The amino acid sequence of the epitope for nmAb-KT evaluated in this study agrees well with our previous study (20), which showed D-44 and K-46 as essential amino acids for the killing activity of HM-1. The absence of D-44 and K-46, in addition to G-41 and T-43, in the HYI sequence can be assumed to be the most probable reason for why HYI does not bind to nmAb-KT.

The variety of techniques used in this study provide a better understanding of both the binding and neutralizing activity of nmAb-KT for HM-1 and HYI. The experimental results obtained and described in this study are useful for determining the epitope for nmAb-KT and can be used as potential tools for further investigations of this antibody as related to its possible clinical applications.

This work was supported by a grant from the Ministry of Education, Science, Sports and Culture of Japan.

#### REFERENCES

1. Starmer, W.T., Ganter, P.F., Aberdeen, V., Lachance, M.A., and Phaff, H.J. (1987) The ecological role of killer yeasts in natural communities of yeasts. *Can. J. Microbiol.* **33**, 783–796

2. Nomoto, H., Kitano, K., Shimazaki, T., Kodama, K., and Hara, S. (1984) Distribution of killer yeasts in the genus *Hansenula*. *Agric. Biol. Chem.* **48**, 807–809
3. Kimura, T., Kitamoto, N., Ohta, Y., Kito, Y., and Iimura, Y.J. (1995) Structural relationships among killer toxins secreted from the killer strains of the genus *Williopsis*. *J. Ferment. Bioeng.* **80**, 85–87
4. Young, T.W. and Yagiu, M. (1978) A comparison of the killer character in different yeasts and its classification. *Antonie Van Leeuwenhoek* **44**, 59–77
5. Ashida, S., Shimazaki, T., Kitano, K., and Hara, S. (1983) New killer toxin of *Hansenula mrakii*. *Agric. Biol. Chem.* **47**, 2953–2955
6. Ohta, Y., Tsukada, Y., and Sugimori, T. (1984) Production, purification and characterization of HYI, an anti-yeast substance, produced by *Hansenula saturnus*. *Agric. Biol. Chem.* **48**, 903–908
7. Yamamoto, T., Hiratani, T., Hirata, H., Imai, M., and Yamaguchi, H. (1986) Killer toxin from *Hansenula mrakii* selectively inhibits cell wall synthesis in a sensitive yeast. *FEBS Lett.* **197**, 50–59
8. Yamamoto, T., Imai, M., Tachibana, K., and Mayumi, M. (1986) Application of monoclonal antibodies to the isolation and characterization of a killer toxin secreted by *Hansenula mrakii*. *FEBS Lett.* **195**, 253–257
9. Anutch, W., Guntert, P., and Wuthrich, K. (1996) Ancestral beta gamma-crystallin precursor structure in a yeast killer toxin. *Nat. Struct. Biol.* **3**, 662–665
10. Kimura, T., Kitamoto, N., Matsuoka, K., Nakamura, K., Iimura, Y., and Kito, Y. (1993) Isolation and nucleotide sequences of the genes encoding killer toxins from *Hansenula mrakii* and *H. saturnus*. *Gene* **137**, 265–270
11. Komiyama, T., Ohta, T., Furuichi, Y., Ohta, Y., and Tsukada, Y. (1995) Structure and activity of HYI killer toxin from *Hansenula saturnus*. *Biol. Pharm. Bull.* **18**, 1057–1059
12. Komiyama, T., Shirai, T., Ohta, T., Urakami, H., Furuichi, Y., Ohta, Y., and Tsukada, Y. (1998) Action properties of HYI killer toxin from *Williopsis saturnus* var. *saturnus*, and antibiotics, aculeacin A and papulacandin B. *Biol. Pharm. Bull.* **21**, 1013–1019
13. Komiyama, T., Ohta, T., Urakami, H., Shiratori, Y., Takasuka, T., Satoh, M., Watanabe, T., and Furuichi, Y. (1996) Pore formation on proliferating yeast *Saccharomyces cerevisiae* cell buds by HM-1 killer toxin. *J. Biochem.* **119**, 731–736
14. Komiyama, T., Zhang, Q.Z., Miyamoto, M., Selvakumar, D., and Furuichi, Y. (2004) Monoclonal antibodies and sandwich ELISA for quantitation of HM-1 killer toxin. *Biol. Pharm. Bull.* **27**, 691–693
15. Kasahara, S., Yamada, H., Mio, T., Shiratori, Y., Miyamoto, C., Yabe, T., Nakajima, T., Ichishima, E., and Furuichi, Y. (1994) Cloning of the *Saccharomyces cerevisiae* gene whose overexpression overcomes the effects of HM-1 killer toxin, which inhibits beta-glucan synthesis. *J. Bacteriol.* **176**, 1488–1499
16. Cabib, E. and Kang, M.S. (1987) Fungal 1,3- $\beta$ -glucan synthase in *Methods in Enzymology* (Ginsberg, V., ed.) **138**, 637–642, Academic press, New York
17. Yamamoto, T., Uchida, K., and Hiratani, T. (1988) In vitro activity of the killer toxin from yeast *Hansenula mrakii* against yeasts and molds. *J. Antibiot.* **XLI**, 398–403
18. Polonelli, L., Lorenzini, R., Bernardis, D.F., and Morace, G. (1986) Potential therapeutic effect of yeast killer toxin. *Mycopathologia* **96**, 103–107
19. Frank, R. (1992) Spot-synthesis: An easy technique for the positionally addressable, parallel chemical synthesis on a membrane support. *Tetrahedron* **48**, 9217–9232
20. Miyamoto, M., Han, G.D., Kimura, T., Furuichi, Y., and Komiyama, T. (2005) Alanine-scanning mutagenesis of HM-1 killer toxin and the essential residues for killing activity. *J. Biochem.* **137**, 517–522